

# Density functional study of ethylene adsorption on palladium clusters

**Citation for published version (APA):**

Fahmi, A., & Santen, van, R. A. (1996). Density functional study of ethylene adsorption on palladium clusters. *Journal of Physical Chemistry*, 100(14), 5676-5680. <https://doi.org/10.1021/jp953002s>

**DOI:**

[10.1021/jp953002s](https://doi.org/10.1021/jp953002s)

**Document status and date:**

Published: 01/01/1996

**Document Version:**

Publisher's PDF, also known as Version of Record (includes final page, issue and volume numbers)

**Please check the document version of this publication:**

- A submitted manuscript is the version of the article upon submission and before peer-review. There can be important differences between the submitted version and the official published version of record. People interested in the research are advised to contact the author for the final version of the publication, or visit the DOI to the publisher's website.
- The final author version and the galley proof are versions of the publication after peer review.
- The final published version features the final layout of the paper including the volume, issue and page numbers.

[Link to publication](#)

**General rights**

Copyright and moral rights for the publications made accessible in the public portal are retained by the authors and/or other copyright owners and it is a condition of accessing publications that users recognise and abide by the legal requirements associated with these rights.

- Users may download and print one copy of any publication from the public portal for the purpose of private study or research.
- You may not further distribute the material or use it for any profit-making activity or commercial gain
- You may freely distribute the URL identifying the publication in the public portal.

If the publication is distributed under the terms of Article 25fa of the Dutch Copyright Act, indicated by the "Taverne" license above, please follow below link for the End User Agreement:

[www.tue.nl/taverne](http://www.tue.nl/taverne)

**Take down policy**

If you believe that this document breaches copyright please contact us at:

[openaccess@tue.nl](mailto:openaccess@tue.nl)

providing details and we will investigate your claim.

# Density Functional Study of Ethylene Adsorption on Palladium Clusters

A. Fahmi\* and R. A. van Santen

Schuit Institute of Catalysis, Laboratory of Inorganic Chemistry and Catalysis, Eindhoven University of Technology, P.O. Box 513, 5600 MB Eindhoven, The Netherlands

Received: October 11, 1995; In Final Form: January 17, 1996<sup>⊗</sup>

Fully optimized geometries and adsorption energies obtained from nonlocal density functional calculations are presented for  $\text{Pd}_n(\text{C}_2\text{H}_4)$  ( $n = 1-6$ ) clusters. The adsorption mode can be  $\pi$  or di- $\sigma$  according to the cluster size. The di- $\sigma$  adsorption mode is characterized by a strong distortion for both the ethylene and the metal cluster. The potential energy surfaces for the C–H activation show that the  $d^{10}$  configuration of palladium is suitable for the formation of the  $\pi$  molecular complexes, whereas the  $d^9s^1$  configuration is suitable for the formation of the  $\sigma$  bonds of the vinyl–hydride products.

## 1. Introduction

In recent years, numerous experimental and theoretical investigations of chemisorption of ethylene on a variety of transition metal surfaces have been carried out utilizing a wide range of techniques. Upon adsorption on a metal surface, ethylene undergoes dehydrogenation–hydrogenation processes that lead to several  $\text{C}_x\text{H}_y$  species on the surface. Despite various experimental studies, reaction mechanisms leading to these species and their localization on the surface are not well determined.

At low temperature (100 K), ethylene is molecularly adsorbed on the metal surface. Two adsorption modes are often discussed: the di- $\sigma$  adsorption mode where ethylene interacts with two metal atoms and the  $\pi$  adsorption mode where ethylene interacts with a single metal atom. High-resolution electron energy loss spectroscopy (HREELS) experiments provide vibrational spectra for adsorbed intermediates on the metal surface. The comparison with the spectra of  $\text{C}_2\text{H}_4\text{Br}_2$  (a model for di- $\sigma$  bonded  $\text{C}_2\text{H}_4$ ), Zeise's salt (a model for  $\pi$ -bonded  $\text{C}_2\text{H}_4$ ), and gaseous  $\text{C}_2\text{H}_4$  allow Stuve and Madix<sup>1</sup> to introduce a  $\pi\sigma$  parameter to characterize the adsorption of  $\text{C}_2\text{H}_4$ . The  $\pi\sigma$  parameter is zero for gaseous  $\text{C}_2\text{H}_4$  and unity for  $\text{C}_2\text{H}_4\text{Br}_2$ . For adsorbed ethylene, the  $\pi\sigma$  parameters for Pd(100),<sup>1</sup> Pd(111),<sup>2</sup> and Pd(110)<sup>3</sup> surfaces are 0.78, 0.43, and 0.39, respectively. These values are attributed to the formation of a di- $\sigma$  complex on Pd(100) and a  $\pi$  complex on Pd(111) and Pd(110) surfaces. Extended Huckel calculations<sup>4,5</sup> have shown that the adsorption mode of ethylene is controlled by a subtle balance between attractive two-electron interactions and repulsive four-electron ones (the Pauli repulsion).

Ethylene behaves differently in the two adsorption modes. At 80 K, the two modes coexist on the Pd(100) surface.<sup>1</sup> While the  $\pi$ -bonded ethylene desorbs upon heating from 100 to 300 K, the di- $\sigma$ -bonded ethylene dehydrogenates into coadsorbed atomic hydrogen and vinyl species. The difference in reactivity should be related to the difference in geometry and electronic structure of ethylene in the two adsorption modes.

In this work, we present a density functional study of the interaction of ethylene with palladium. Clusters of 1–6 metal atoms are used. The two adsorbed ethylene species  $\pi$  and di- $\sigma$  are described. The activation of the C–H bond of ethylene is analyzed for the single atom and the dimer. One of the main aspects of our calculations is a full geometry optimization of the whole system  $\text{C}_2\text{H}_4/\text{Pd}_n$ . This approach is different from

the common approach that consists in freezing the cluster, which is supposed to simulate a metal surface, and optimizing the adsorbate. On one hand our approach will give information about the magnitude of the local relaxation induced by the adsorption of ethylene on the palladium surface. On the other hand, our calculations should describe the interaction of ethylene with palladium clusters in the gas phase. The calculation method is described in section 2. The molecular properties of the bare  $\text{Pd}_n$  clusters are presented in section 3. Adsorption and activation of the C–H bond by the palladium single atom and dimer are discussed in sections 4 and 5, respectively. Section 6 is devoted to the evolution of the ethylene adsorption with the cluster size.

## 2. Method of Calculation

A density functional method is used to determine geometries, adsorption energies, and transition states for the  $\text{C}_2\text{H}_4/\text{Pd}_n$  ( $n = 1-6$ ) systems. We have performed quasi-relativistic spin-unrestricted, frozen-core calculations using the Amsterdam Density Functional (ADF) program.<sup>6</sup> The program represents the molecular orbitals as linear combinations of atomic Slater-type orbitals and solves the Kohn–Sham one-electron equations using the Vosko–Wilk–Nusair<sup>7</sup> local spin density approximation (LDA). To correct the overbinding inherent to LDA, nonlocal gradient corrections for the exchange (Becke functional<sup>8</sup>) and correlation (Perdew functional<sup>9</sup>) terms were computed self-consistently. Relativistic effects were taken into account by first-order perturbation theory.<sup>10</sup> For the carbon atom, a frozen core potential is used for the 1s electrons; for the palladium atom, electrons up to the 4p shell are frozen. The basis sets are of double- $\zeta$  quality except the palladium d orbitals which are triple- $\zeta$ .

Adsorption energies have been calculated according to the expression:

$$E_{\text{ads}} = E_{(\text{C}_2\text{H}_4/\text{Pd}_n)} - (E_{\text{Pd}_n} + E_{\text{C}_2\text{H}_4})$$

where  $E_{\text{Pd}_n}$  and  $E_{\text{C}_2\text{H}_4}$  are total energies of the bare cluster and ethylene, respectively, and  $E_{(\text{C}_2\text{H}_4/\text{Pd}_n)}$  is the total energy of the adsorbate/substrate system. A negative  $E_{\text{ads}}$  value corresponds to a stable adsorbate/substrate system.

## 3. Bare $\text{Pd}_n$ ( $n = 1-6$ ) Clusters

**3.1. The Palladium Single Atom.** As a reference point, we have calculated the splitting between the two lowest states

<sup>⊗</sup> Abstract published in *Advance ACS Abstracts*, March 1, 1996.

**TABLE 1: Molecular Properties for the Triplet and Singlet States of the Palladium Dimer**

Pd <sub>2</sub> state	binding energy (kcal/mol)	Pd–Pd (Å)	frequency (cm <sup>-1</sup> )	Mulliken populations: s/p/d
triplet	-29	2.56	213	0.55/0.02/9.43
singlet	-25	2.74	187	0.17/0.02/9.80

**TABLE 2: Molecular Properties of the Pd<sub>n</sub> Bare Clusters**

Pd <sub>n</sub>	atomic coordination	Mulliken populations: s/p/d	Pd–Pd (Å)	Pd–Pd bond strength (kcal/mol)
1		0/0/10		
2	1	0.55/0.02/9.43	2.56	29.2
3 <i>D</i> <sub>3h</sub>	2	0.66/0.03/9.31	2.76	27.2
4 <i>T</i> <sub>d</sub>	3	0.54/0.04/9.42	2.75	26.2
5 <i>D</i> <sub>3h</sub>	3 (top)	0.42/0.04/9.56	2.79	23.9
	4 (base)	0.52/0.04/9.42		
6 <i>O</i> <sub>h</sub>	4	0.46/0.04/9.50	2.78	23.6

of the palladium single atom. The calculated energy difference between the <sup>1</sup>S(d<sup>10</sup>) ground state and the <sup>3</sup>D(d<sup>9</sup>s<sup>1</sup>) excited state is 26 kcal/mol; the experimental value is 22 kcal/mol.<sup>11</sup>

**3.2. The Palladium Dimer.** In agreement with previous theoretical calculations (Hartree-Fock<sup>12</sup> and DFT<sup>13</sup>), we found the ground state of the palladium dimer to be triplet. The calculated molecular properties are summarized in Table 1 for the triplet and the singlet states. Bonding energies are relative to two Pd(d<sup>10</sup>) atoms. The triplet state is more stable by 4 kcal/mol. The estimated experimental bonding energy for the dimer is between 16 and 26 kcal/mol<sup>14</sup> according to the technique of evaluation. The Mulliken population analysis shows that the singlet state is composed of two interacting d<sup>10</sup> atoms. The Pd–Pd bond length is shorter and the vibrational frequency is higher for the triplet state.

**3.3. The Pd<sub>n</sub> (n = 3–6) Bare Clusters.** For the Pd<sub>n</sub> (n = 3–6) bare clusters, only compact structures were investigated. A density functional analysis of the structure of small palladium clusters show that compact structures are more stable than open structures, and states of triplet spin are more stable than states of singlet spin.<sup>15</sup> Our calculations show that for Pd<sub>3</sub>, the triangular geometry (*D*<sub>3h</sub>) is more stable by 29 kcal/mol relative to the linear geometry (*D*<sub>∞h</sub>). For small clusters, the atomic arrangements are controlled by local bonding and orbital overlapping rather than long-range interaction as it is in the bulk structure. Cluster geometries are cluster size dependent and experimental structure determinations often proceed via indirect methods (for instance N<sub>2</sub> adsorption for the determination of the structures of Ni<sub>n</sub> clusters<sup>16</sup>). The other investigated geometries are Pd<sub>4</sub> (*T*<sub>d</sub>), Pd<sub>5</sub> (*D*<sub>3h</sub>), and Pd<sub>6</sub> (*O*<sub>h</sub>). The calculated properties are shown in Table 2. All these clusters present ground states of spin triplet, previous DFT, or Hartree–Fock studies of Pd<sub>3</sub><sup>17</sup> and Pd<sub>4</sub><sup>18</sup> clusters have shown that these clusters are indeed triplet. The optimized Pd–Pd bond remains close to the bulk value, 2.75 Å.<sup>19</sup> The Pd–Pd bond strength decreases with the cluster size but is still far from the experimental value, 15 kcal/mol.<sup>19</sup> The Mulliken populations (for n = 3, 4, 6) show a decrease of the s electrons and increase of the d electrons with the cluster size. The energy band calculation for the palladium bulk structure<sup>20</sup> gives 0.37 and 9.63 electrons for the valence s and d orbitals, respectively.

#### 4. The Pd(C<sub>2</sub>H<sub>4</sub>) Complex

The Pd(C<sub>2</sub>H<sub>4</sub>) complex was first synthesized by Ozin and Power<sup>21</sup> using C<sub>2</sub>H<sub>4</sub>/Xe matrices. This complex has also been subject of theoretical investigations. Blomberg et al., using an ab initio Hartree–Fock method, calculated the bonding energy

**TABLE 3: Adsorption Energies (kcal/mol) Relative to Free Species and Geometries (Å and deg) for the Molecular Complex, the Transition State, and the Vinyl–Hydride Product of the Pd(C<sub>2</sub>H<sub>4</sub>) Complex<sup>a</sup>**

	Pd(C <sub>2</sub> H <sub>4</sub> )	transition state	H–Pd–C <sub>2</sub> H <sub>3</sub>
<i>E</i> <sub>ads</sub>	-39		-6
C–C	1.40	1.32	1.34
Pd–C	2.20	2.00	1.98
Pd–H	2.72	1.68	1.57
H–Pd–C	106	54	78

<sup>a</sup> For the transition state, the barrier height relative to the π complex is 36 kcal/mol.

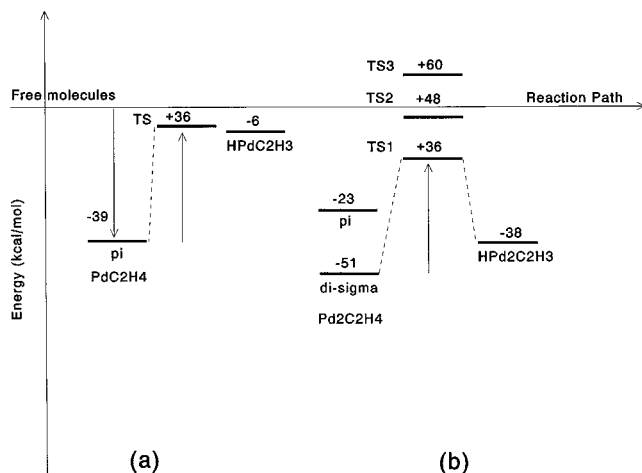


**Figure 1.** Potential energy surfaces for the activation of the C–H bond of ethylene by the palladium single atom (a) and dimer (b); the reference for adsorption energies (in kcal/mol) corresponds to free molecules (Pd + C<sub>2</sub>H<sub>4</sub> or Pd<sub>2</sub> + C<sub>2</sub>H<sub>4</sub>) in their equilibrium geometries. For the transition states the barrier heights (relative to π and di-σ adsorption for Pd and Pd<sub>2</sub>, respectively) are indicated. TS1, TS2, and TS3 for Pd<sub>2</sub>C<sub>2</sub>H<sub>4</sub>, correspond to the side-on parallel, side-on perpendicular, and end-on approaches (see Figure 3).

of the complex<sup>22</sup> and the activation of the C–H bond of ethylene by the palladium single atom.<sup>23</sup>

During the interaction of ethylene with a transition metal donation and back-donation processes take place. The donation involves a transfer of electrons from the ethylene π orbital to the metal unoccupied orbitals, whereas the back-donation populates the ethylene π\* orbital with electrons from the occupied metal orbitals. This is the well-known Dewar–Chatt–Duncanson mechanism.<sup>24</sup> Both donation and back-donation are attractive interactions. The repulsion (Pauli repulsion) is due to the interaction between the occupied orbitals of ethylene and the transition metal. The first consequence of the donation and back-donation processes is the weakening of the C–C bond strength, the bond length increases from 1.34 Å in the gas phase to 1.40 Å in the complex. The formation of the Pd–C bonds induces a small rehybridization of the carbon atom from sp<sup>2</sup> toward sp<sup>3</sup> (see Table 3). The dihedral angle between the HCC plane and the CCPd plane increases from 90° to 98°; for a complete sp<sup>3</sup> hybridization, this angle should be 120°. The ground state of the complex is singlet with a bonding energy of -39 kcal/mol. This value is close to that calculated by Blomberg et al.,<sup>22</sup> -31 kcal/mol. The overall charge transfer is a back-donation of 0.07 electrons to ethylene. The donation to the metal is small, 0.01 electrons.

The potential energy surface for the activation of the C–H bond is shown in Figure 1. The most interesting aspect of this potential is perhaps that the transition state is below the Pd + C<sub>2</sub>H<sub>4</sub> asymptote; the energy difference to the asymptote is 3 kcal/mol. The barrier height is 36 kcal/mol and the energy

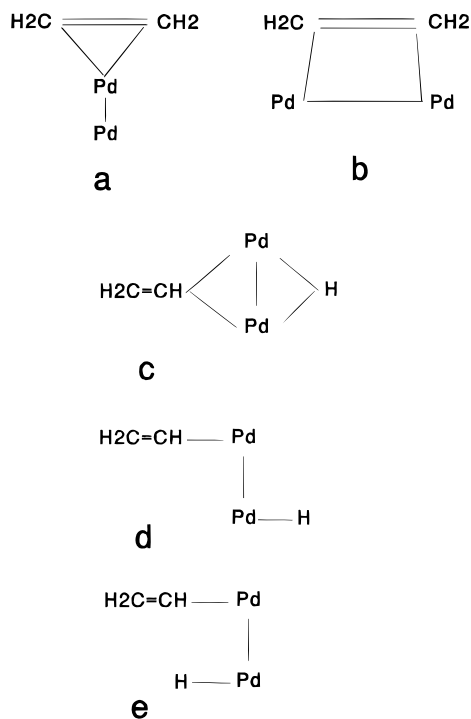


**Figure 2.** Adsorption modes of ethylene on Pd<sub>2</sub>, (a)  $\pi$  and (b) di- $\sigma$ , and various geometries for the vinyl-hydride product, (c) pseudo-square planar, (d) trans, and (e) cis.

difference between the transition state and the vinyl-hydride product is small, 6 kcal/mol. Our results are in good agreement with Siegbahn et al.<sup>23</sup> calculations, which found a barrier height of 31 kcal/mol and an energy difference of 3 kcal/mol between the transition state and the vinyl hydride product.

### 5. Interaction of Ethylene with the Palladium Dimer

Two kind of complexes can be formed (Figure 2, parts a and b):  $\pi$  and di- $\sigma$  complexes. The molecular properties of the two complexes are presented in Table 4. The di- $\sigma$  complex is more stable and is characterized by a large charge transfer from the dimer to ethylene (back-donation). The di- $\sigma$  adsorption mode gives a strong interaction and a strong distortion of ethylene toward the  $sp^3$  hybridization, whereas the  $\pi$  adsorption mode gives a small interaction and a small distortion. The same trend was found by Extended Huckel calculations for the adsorption of C<sub>2</sub>H<sub>4</sub> on Pd(111) and Pt(111) surfaces.<sup>4</sup> Table 4 also shows the decomposition of the interaction energy of ethylene with the dimer. The interaction energy is decomposed in three contributions:<sup>25</sup> the Pauli repulsion  $\Delta E_p$ , the electrostatic interaction  $\Delta E_{elec}$ , and the orbital interaction  $\Delta E_{orb}$ . The Pauli repulsion arises from the interaction between occupied orbitals of C<sub>2</sub>H<sub>4</sub> and Pd<sub>2</sub>; the electrostatic interaction corresponds to the interpenetrating charge distributions; and the orbital interaction represents the energy change upon the formation of the molecular orbitals of the C<sub>2</sub>H<sub>4</sub>/Pd<sub>2</sub> system. This energy calculated with the Ziegler transition-state method<sup>25d</sup> for the optimized adsorbate/substrate system corresponds to the interaction between two distorted fragments and is not the adsorption energy that refers to free molecules in their equilibrium geometries (the sum  $\Delta E_p + \Delta E_{elec} + \Delta E_{orb}$  is not equal to  $E_{ads}$ ). The Pauli repulsion is stronger for the di- $\sigma$  adsorption. However, the compensation by the other contributions is large enough to favor the di- $\sigma$  adsorption mode.

We have also analyzed the activation of the C-H bond of ethylene by the palladium dimer. Three structures for the vinyl-hydride product (H-Pd<sub>2</sub>-C<sub>2</sub>H<sub>3</sub>) were investigated: the

pseudo-square planar structure (Figure 2c, the vinyl plane is perpendicular to the plane containing the two Pd atoms and the hydrogen atom), the trans (Figure 2d) and the cis (Figure 2e) structures. The optimized parameters are given in Table 5. The square structure is the most stable structure, therefore the vinyl-hydride H-Pd<sub>2</sub>-C<sub>2</sub>H<sub>3</sub> presents a square geometry equivalent to that of H-Pd<sub>2</sub>-CH<sub>3</sub> resulting from CH<sub>4</sub> activation.<sup>17</sup> On the other hand, because of the steric repulsion, the cis structure is less stable than the trans structure by 4 kcal/mol.

The potential energy surface for the activation of the C-H bond by the palladium dimer is presented in Figure 1 together with that of the single atom. The comparison of the stability of the  $\pi$  complexes and vinyl-hydride products of PdC<sub>2</sub>H<sub>4</sub> and Pd<sub>2</sub>C<sub>2</sub>H<sub>4</sub> (see Figure 1) shows that the d<sup>10</sup> configuration (the palladium single atom) is optimal for the formation of the  $\pi$  complex, whereas the d<sup>9</sup>s<sup>1</sup> configuration (that of Pd<sub>2</sub> is d<sup>9.43</sup>s<sup>0.55</sup>) should be optimal for the formation of the  $\sigma$ -bonds of the vinyl-hydride product. Indeed, the PdC<sub>2</sub>H<sub>4</sub>  $\pi$ -complex is stable by 39 kcal/mol relative to free molecules in their ground states, whereas the Pd<sub>2</sub>C<sub>2</sub>H<sub>4</sub>  $\pi$ -complex is stable only by 23 kcal/mol. On the other hand, the vinyl-hydride H-Pd-C<sub>2</sub>H<sub>3</sub> is stable only by 6 kcal/mol, whereas H-Pd<sub>2</sub>-C<sub>2</sub>H<sub>4</sub> is stable by 38 kcal/mol.

Three transition states were investigated (Figure 3). In the end-on approach (TS3), the Pd-Pd axis is perpendicular to the C-H bond and only one Pd atom is involved in the interaction. The other Pd atom is kept far from ethylene. In the side-on perpendicular approach (TS2), the two molecules are parallel and the Pd-Pd axis is kept perpendicular to the C-H bond. For the side-on parallel approach (TS1), the Pd-Pd axis is kept parallel to the C-H bond. When only one Pd atom of the dimer activates the C-H bond (TS3), the calculated barrier relative to  $\pi$  adsorption is very close to that of the single atom (37 vs 36 kcal/mol). The barrier relative to di- $\sigma$  adsorption is larger, 60 kcal/mol, and is a consequence of the energy difference between  $\pi$  and di- $\sigma$  adsorption modes. The side-on perpendicular approach was found for the activation of N<sub>2</sub><sup>26</sup> and CH<sub>4</sub><sup>17</sup> by Pd<sub>2</sub>. The transition state (TS2) is characterized by a long Pd-Pd distance (2.92 Å). While the vinyl group is attached to the two Pd atoms, the hydrogen atom is attached to the vinyl and to one Pd atom. The barrier is 48 kcal/mol. The side-on parallel approach was suggested by Nakatsuji et al.<sup>27</sup> for the activation of H<sub>2</sub> by Pd<sub>2</sub>. Then the final product H-Pd-Pd-H presents a cis configuration. Blomberg et al.<sup>17</sup> have found that the square configuration, where each hydrogen is attached to the two Pd atoms, is more stable by 26 kcal/mol. Therefore the side-on parallel approach is not necessarily the optimal pathway for H-H activation on Pd<sub>2</sub>. The transition state (TS1) for C<sub>2</sub>H<sub>4</sub>/Pd<sub>2</sub> side-on parallel approach gives the lowest barrier relative to di- $\sigma$  adsorption, 36 kcal/mol. The main reason seems to be the participation of the second carbon atom in the interaction with the dimer, which is missing in the other transition states. The topology of the transition state is close to the di- $\sigma$  adsorption. The inactive CH<sub>2</sub> group remains attached to one Pd atom, while the activation takes place on the other Pd atom. Here again the activation is ensured by only one Pd atom; therefore, the barrier is equal to that of the single atom.

Our calculations show clearly that the palladium single atom and dimer activate the ethylene C-H bond. This result supports molecular beam experiments from Fayet et al.<sup>28</sup> where palladium clusters with up to 25 atoms were found to activate ethylene. However, while in these experiments the dimer is more reactive than the single atom, in our calculations Pd<sub>2</sub> and Pd present the same barrier height.

**TABLE 4: Adsorption Energies (in kcal/mol) Relative to Free C<sub>2</sub>H<sub>4</sub> and Pd<sub>2</sub> Species, the Decomposition of the Interaction Energy between C<sub>2</sub>H<sub>4</sub> and Pd<sub>2</sub> for the Optimized C<sub>2</sub>H<sub>4</sub>/Pd<sub>2</sub> Geometry,<sup>a</sup> Overall Charge Transfer (a Back-Donation to Ethylene), and Geometries (Å and deg) for  $\pi$  and di- $\sigma$  Complexes of Pd<sub>2</sub>(C<sub>2</sub>H<sub>4</sub>)<sup>b</sup>**

adsorption mode	$E_{\text{ads}}$	$\Delta E_{\text{D}}$	$\Delta E_{\text{elec}}$	$\Delta E_{\text{orb}}$	charge transfer	Pd-Pd	Pd-C	C-C	hydrogen dihedral angle
$\pi$	-23	+161	-141	-56	0.09 e <sup>-</sup>	2.86	2.22	1.40	99
di- $\sigma$	-51	+231	-195	-111	0.14 e <sup>-</sup>	2.74	2.12	1.44	107

<sup>a</sup>  $\Delta E_{\text{p}}$ , Pauli repulsion;  $\Delta E_{\text{elec}}$ , electrostatic interaction;  $\Delta E_{\text{orb}}$ , orbital interaction. <sup>b</sup> The hydrogen dihedral angle is the angle between the HCC and the CCPd planes.

**TABLE 5: Ethylene Dissociation on Pd<sub>2</sub><sup>a</sup>**

structure	$E_{\text{ads}}$ or barrier height	Pd <sub>1</sub> -Pd <sub>2</sub>	Pd <sub>1</sub> -C/Pd <sub>2</sub> -C	Pd <sub>1</sub> -H/Pd <sub>2</sub> -H	C-H	C-C
HPd <sub>2</sub> C <sub>2</sub> H <sub>3</sub>						
square	-38	2.78	2.10	1.73	1.73	1.36
trans	-13	2.66	1.96	1.56	1.56	1.36
cis	-9	2.67	1.96	1.54	1.54	1.34
transition state						
end-on	60	2.81	2.00	1.53	1.53	1.32
side-on perpendicular	48	2.92	2.12/2.13	1.63/2.44	1.60	1.36
side-on parallel	36	2.81	2.16/2.30	1.61/3.53	1.65	1.40

<sup>a</sup> The adsorption energies (in kcal/mol) for the vinyl-hydride product are relative to free C<sub>2</sub>H<sub>4</sub> and Pd<sub>2</sub> species; the barrier heights (in kcal/mol) for the transition states are relative to the di- $\sigma$  molecular complex; and the distances are in Å.

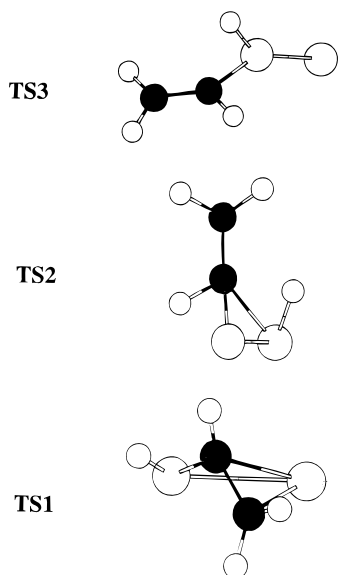


**Figure 3.** Various transition states for the C-H activation by Pd<sub>2</sub>: TS1, side-on parallel approach; TS2, side-on perpendicular approach; and TS3, end-on approach.

## 6. Adsorption of Ethylene on Pd<sub>n</sub> (n = 3-6) Clusters

In this section, we present the results for the adsorption of ethylene on Pd<sub>n</sub> (n = 3-6) clusters. The two adsorption modes  $\pi$  and di- $\sigma$  are studied. The most surprising result is the change in the cluster structure associated with the di- $\sigma$  adsorption mode. For Pd<sub>n</sub> (n = 3-5) clusters, the bond between the two Pd atoms involved in the adsorption is broken (see Figure 4). Ethylene induces a reconstruction of the clusters: from the triangle toward the linear structure for Pd<sub>3</sub> and from the tetrahedron toward the planar structure for Pd<sub>4</sub>. Such effects were already suggested by Parks et al.<sup>16</sup> for N<sub>2</sub> adsorption on Ni<sub>n</sub> clusters. In their investigation of the structure of nickel clusters, they have found that in some cases nitrogen causes a change in the cluster structure. In Figure 4 we notice that the Pd-Pd distance and therefore the distortion decreases with the cluster size. Therefore this effect will be weak on the palladium surface and will correspond to a local relaxation of the surface. The structural effect associated with the  $\pi$  adsorption mode is smaller, and there is an increase of the bond length between the atom involved in the adsorption and its first neighbors. This is a general trend for the adsorption on a transition metal surface,

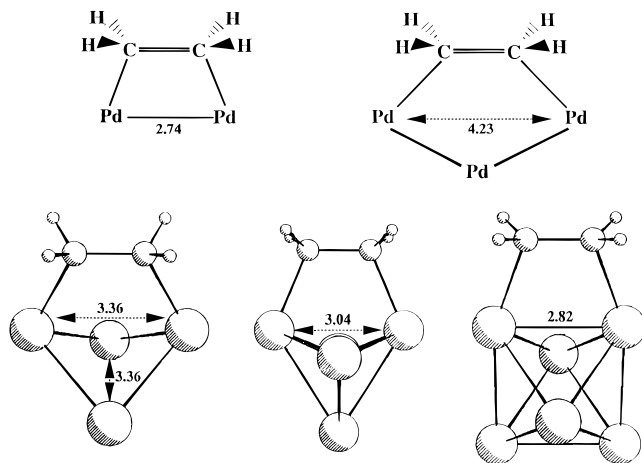


**Figure 4.** Cluster distortion under the di- $\sigma$  adsorption mode (distances in Å).

**TABLE 6: Structures of  $\pi$  and Di- $\sigma$  C<sub>2</sub>H<sub>4</sub>Pd<sub>n</sub> Complexes<sup>a</sup>**

Pd <sub>n</sub>	spin		Pd-Pd		C-C		hydrogen dihedral angle	
	$\pi$	di- $\sigma$	$\pi$	di- $\sigma$	$\pi$	di- $\sigma$	$\pi$	di- $\sigma$
1	S	S			1.40		98	
2	T	S	2.86	2.74	1.40	1.44	99	107
3	T	S	2.77	4.22	1.39	1.43	98	109
4	T	S	2.82	3.36	1.38	1.46	97	114
5	T	S	2.81	3.04	1.39	1.46	99	113
6	T	T	2.83	2.82	1.39	1.42	98	105

<sup>a</sup> Spin (S for singlet and T for triplet), Pd-Pd distance (Å) of atoms involved in the adsorption and the geometry of adsorbed ethylene (Å and deg).

and metal atoms involved in the adsorption are often pulled out from the surface.

For the distortion of adsorbed ethylene (Table 6), we found the same trend as for the dimer, a higher distortion (rehybridization) for the di- $\sigma$  adsorption mode. The C-C bond length is longer when C<sub>2</sub>H<sub>4</sub> is di- $\sigma$ . A comparison can be made with the benzene adsorption on Rh(111), LEED analysis<sup>29</sup> has shown that the benzene is adsorbed on a 3-fold position, and then, half of the C-C bonds are on top positions and the other half are on bridge positions. In correlation with our results, the C-C bond on top (equivalent to a  $\pi$  adsorption) is shorter than the C-C bond on bridge (equivalent to a di- $\sigma$  adsorption). The experimental value of the C-C bond for adsorbed ethylene on

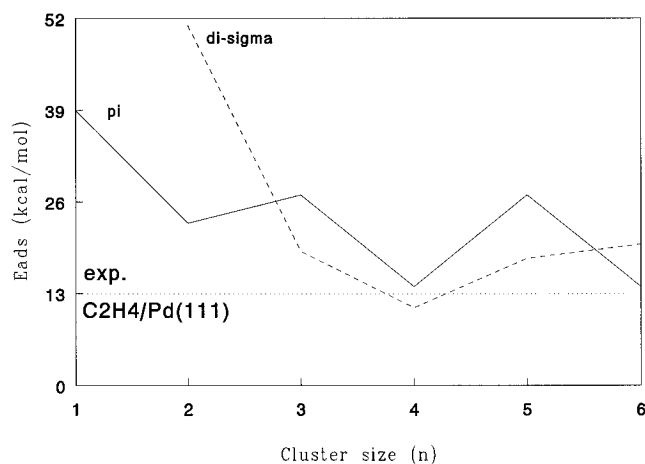


**Figure 5.** Evolution of the ethylene adsorption with the cluster size  $\text{Pd}_n$  ( $n = 1-6$ ).

$\text{Pd}(111)$ ,<sup>30</sup> 1.43 Å, is close to the calculated values for the di- $\sigma$  adsorption mode, 1.42–1.46 Å. However, HREELS experiments support a  $\pi$  adsorption on  $\text{Pd}(111)^2$  and  $\text{Pd}(110)$ ,<sup>3</sup> whereas for  $\text{Pd}(100)^1$  both  $\pi$  and di- $\sigma$  modes were observed. Table 6 also shows the spin state of the  $\text{C}_2\text{H}_4\text{Pd}_n$  complexes. In the di- $\sigma$  adsorption, the reaction between ethylene and the cluster can be described as an oxidative addition reaction in which the  $\pi$  bond of ethylene is broken and two metal–carbon  $\sigma$  bonds are formed. Therefore all the di- $\sigma$  complexes are singlet except the  $\text{C}_2\text{H}_4\text{Pd}_6$  complex where the distortion of ethylene is the smallest. The distortion of ethylene is smaller in the  $\pi$  adsorption and the spin of the cluster is not perturbed. Therefore all the  $\pi$  complexes except the  $\text{C}_2\text{H}_4\text{Pd}$  complex are triplet. The latter is singlet because the single atom  $\text{Pd}(d^{10})$  is singlet.

The evolution of the adsorption energy with the cluster size is sketched in Figure 5. The adsorption energy oscillates and decreases with the cluster size toward the experimental value, 13 kcal/mol.<sup>31</sup> Chemical physics of gas-phase clusters<sup>28,32</sup> show that reactive properties of small metal clusters are different from those of the bulk. In some cases the change in the cluster size by one metal atom can be accompanied by a large change in the reactivity, and curves like Figure 5 were often found in experiments. We notice that for  $\text{Pd}_{3-5}$  clusters, which collapse under the di- $\sigma$  adsorption, the best adsorption mode is  $\pi$ , whereas the  $\text{Pd}_2$  and  $\text{Pd}_6$ , which give  $\pi$  and di- $\sigma$  distortions of the same magnitude, the di- $\sigma$  adsorption is more favorable.

## 7. Conclusion

In this work we have presented density functional calculations on the adsorption of ethylene on small palladium clusters,  $\text{Pd}_n$  ( $n = 1-6$ ). The adsorption mode can be  $\pi$  or di- $\sigma$  according to the cluster size. The adsorption energy oscillates and decreases with the cluster size toward the experimental value. The  $\pi$  adsorption is maximum for the single atom, whereas the di- $\sigma$  adsorption is maximum for the dimer.  $\text{Pd}_n$  ( $n = 3-5$ ) clusters are not stable against adsorption, they undergo structural changes to accommodate ethylene. The Pd–Pd bond for atoms involved in the di- $\sigma$  adsorption is broken. Ethylene shows a stronger rehybridization with the di- $\sigma$  adsorption, the C–C bond length and the hydrogen dihedral angle are large compared with the values obtained with the  $\pi$  adsorption. Both the single atom and the dimer activate the C–H bond of ethylene in agreement with the molecular beam experiments in the gas phase. The potential energy surfaces are characterized by very stable molecular complexes compared with vinyl–hydride products. These potentials show that the  $d^{10}$  configuration (the single atom)

is appropriate for the  $\pi$  interaction, whereas the  $d^9s^1$  configuration is appropriate for the di- $\sigma$  interaction (the dimer is  $d^{9.43}s^{0.55}$ ).

**Acknowledgment.** We thank Dr. Matthew Neurock for fruitful discussions. We thank the theoretical group of the Free University of Amsterdam for the use of the ADF program. This work was supported by the Eindhoven University of Technology. We kindly acknowledge the computational resources allocated from the National Computing Facilities (NCF) Foundation under project SC-183.

## References and Notes

- (1) Stuve, E. M.; Madix, R. J. *J. Phys. Chem.* **1985**, *89*, 105.
- (2) Gates, J. A.; Kesmodel, L. L. *Surf. Sci.* **1982**, *120*, L461.
- (3) Nishijima, M.; Yoshinobu, J.; Sekitani, T.; Onichi, M. *J. Chem. Phys.* **1989**, *90*, 5114.
- (4) Sautet, P.; Paul, J. F. *Catal. Lett.* **1991**, *9*, 245.
- (5) Sautet, P.; Paul, J. F. *J. Phys. Chem.* **1994**, *98*, 10906.
- (6) (a) Baerends, E. J.; Elis, D. E.; Ros, P. *Chem. Phys.* **1973**, *2*, 41. (b) Boerrigter, P. M.; te Velde, G.; Baerends, E. J. *Int. J. Quantum Chem.* **1988**, *33*, 87. (c) Baerends, E. J.; Ros, P. *Int. J. Quantum Chem.: Quantum Chem. Symp.* **1978**, *12*, 169.
- (7) Vosko, S. H.; Wilk, L.; Nusair, M. *Can. J. Phys.* **1980**, *58*, 1200.
- (8) Becke, A. D. *Phys. Rev. A* **1988**, *38*, 3098. Becke, A. D. *ACS Symp. Ser.* **1989**, *394*, 165.
- (9) Perdew, J. P. *Phys. Rev. B* **1986**, *33*, 8822.
- (10) Snijders, J. G.; Baerends, E. J. *Mol. Phys.* **1978**, *36*, 1789. Snijders, J. G.; Baerends, E. J. *Mol. Phys.* **1979**, *38*, 1909.
- (11) Blomberg, M. R. A.; Lebrilla, C. B.; Siegbahn, P. E. M. *Chem. Phys. Lett.* **1988**, *150*, 522.
- (12) Balasubramanian, K. *J. Chem. Phys.* **1988**, *89*, 6310.
- (13) Nakao, T.; Dixon, D. A. *J. Phys. Chem.* **1993**, *97*, 12665.
- (14) Lin, S.-S.; Strauss, B.; Kant, A. *J. Chem. Phys.* **1969**, *51*, 2282.
- (15) Neurock, M.; Dixon, D. A.; Coulston, G. W. Manuscript in preparation.
- (16) Parks, E. K.; Zhu, L.; Riley, S. J. *J. Chem. Phys.* **1994**, *100*, 7206.
- (17) Blomberg, M. R. A.; Siegbahn, P. E. M.; Svensson, M. *J. Phys. Chem.* **1992**, *96*, 5783.
- (18) (a) Miyoshi, E.; Sakai, Y.; Mori, S. *Chem. Phys. Lett.* **1985**, *113*, 457. (b) Goursoot, A.; Papai, I.; Salahub, D. R. *J. Am. Chem. Soc.* **1992**, *114*, 7452. (c) Dai, D.; Balasubramanian, K. *J. Chem. Phys.* **1995**, *103*, 648.
- (19) *Handbook of Chemistry and Physics*; West, R. C., Ed.; CRC: Cleveland, 1986.
- (20) Anderson, O. K. *Phys. Rev. B* **1970**, *2*, 883.
- (21) Ozin, G. A.; Power, W. J. *Inorg. Chem.* **1977**, *16*, 212.
- (22) Blomberg, M. R. A.; Siegbahn, P. E. M.; Svensson, M. *J. Phys. Chem.* **1992**, *96*, 9794.
- (23) Siegbahn, P. E. M.; Blomberg, M. R. A.; Svensson, M. *J. Am. Chem. Soc.* **1993**, *115*, 1952.
- (24) (a) Dewar, M. J. S. *Bull. Soc. Chim. Fr. C* **1950**, *71*, 18. (b) Chatt, J.; Duncanson, L. A. *J. Chem. Soc. London* **1953**, 2939.
- (25) (a) Post, D.; Baerends, E. J. *J. Chem. Phys.* **1983**, *78*, 5663. (b) Baerends, E. J.; Rozendaal, A. In *Quantum Chemistry: The Challenge of Transition Metals and Coordination Chemistry*; Veillard, A., Ed.; NATO-ASI Series; Reidel: Dordrecht 1986; p 159. (c) van den Hoek, P. J.; Kleyn, A. W.; Baerends, E. J. *Comments At. Mol. Phys.* **1989**, *23*, 93. (d) Ziegler, T.; Rauk, A. *Theor. Chim. Acta* **1977**, *46*, 1.
- (26) Blomberg, M. R. A.; Siegbahn, P. E. M. *Chem. Phys. Lett.* **1991**, *179*, 524.
- (27) Nakatsuji, H.; Hada, M.; Yonezawa, T. *J. Am. Chem. Soc.* **1987**, *109*, 1902.
- (28) Fayet, T.; Kaldor, A.; Cox, D. M. *J. Chem. Phys.* **1990**, *92*, 254.
- (29) Barbieri, A.; vanHove, M. A.; Somorjai, G. A. *Surf. Sci.* **1994**, *306*, 261.
- (30) Wang, L. P.; Tysoc, W. T.; Ormerod, R. M.; Lamberts, R. M.; Hoffmann, H.; Zaera, F. *J. Phys. Chem.* **1990**, *94*, 4236.
- (31) Tysoc, W. T. *J. Phys. Chem.* **1984**, *88*, 1963.
- (32) (a) Cox, D. M.; Kaldor, A.; Fayet, P.; Eberhardt, W.; Brickman, R.; Sherwood, R.; Fu, Z.; Sondericher, D. In *Novel Materials in Heterogeneous Catalysis*; Terry, R., Baker, K., Murrell, L., Eds.; ACS: Washington, DC, 1990; p 172. (b) Kaldor, A.; Cox, D. M. *J. Chem. Soc., Faraday Trans.* **1990**, *86*, 2459. (c) Trevor, D. J.; Cox, D. M.; Kaldor, A. *J. Am. Chem. Soc.* **1990**, *112*, 3742.